https://doi.org/10.5194/cp-2022-29
Preprint. Discussion started: 20 April 2022


Climate of the Past Discussions

# Paleoclimatic value of sediment pixel intensity time series from Lago Argentino, Patagonia

Maximillian Van Wyk de Vries[1,2], Emi Ito[1,3], Mark Shapley[3], Matias Romero[4,5], and Guido Brignone[4]

[1]Department of Earth and Environmental Sciences, University of Minnesota, Minneapolis, MN 55455, USA.
[2]Saint Anthony Falls Laboratory, University of Minnesota, Minneapolis, MN 55455, USA.
[3]Continental Scientific Drilling Facility, Dept. of Earth and Environmental Sciences, University of Minnesota, Minneapolis, MN 55455, USA.
[4]Facultad de Ciencias Exactas, Físicas y Naturales (FCEFyN), Universidad Nacional de Córdoba, Av. Haya de la Torre, Córdoba, X5000HUA, Argentina.
[5]Centro de Investigaciones en Ciencias de la Tierra (CICTERRA), Consejo Nacional de Investigaciones Científicas y Tecnológicas (CONICET), Córdoba, X5000IND, Argentina.

**Correspondence:** Maximillian Van Wyk de Vries (vanwy048@umn.edu)

**Abstract.** The quantity and characteristics of sediment deposited in lakes are affected by climate to varying extents. As sediment is deposited, it provides a record of past climatic or environmental conditions. However, determining a direct relationship between specific climatic variables and measurable sediment properties, for instance between temperature and sediment optical reflectance, is complex. In this study, we investigate the suitability of sediment reflectance, recorded as digital pixel intensity (PxI), as a paleoclimate proxy at a large ice-contact lake in southern Patagonia, Lago Argentino. We also evaluate whether sediment PxI can be used to investigate the present-day climatic drivers of sedimentation across Lago Argentino. First, we show that sediment PxIs relate to underlying sediment composition, and are significantly correlated with XRF major element compositional data. Secondly, we find that PxIs correlate with both austral summer temperatures and austral summer wind speeds, but not with precipitation. PxI timeseries reach the correlation significance threshold for use as paleo-temperature or paleo-wind speed proxies. However, high spatial variability and the non-unique relationship between PxI and both temperature and wind speed challenges the necessary assumption of stationarity at Lago Argentino. While we do not find it suitable for use as a paleoclimatic proxy, significant correlations between PxI and instrumental climate data do chronicle current climatic controls on sediment deposition at Lago Argentino: high summer temperatures enhance settling of coarse, optically dark grains across the lake basin by promoting ice melt and lake stratification, while high wind speeds reduce the settling of fine, optically bright grains in the ice-proximal regions by transporting sediment-rich waters away from the glacier fronts. The assumptions required for quantitative paleoclimatic reconstruction must be carefully evaluated in complex lacustrine environments, but records unsuitable for use as proxies might nevertheless yield valuable information about the drivers of modern sedimentary transport and deposition.

https://doi.org/10.5194/cp-2022-29
Preprint. Discussion started: 20 April 2022

Climate of the Past Discussions

## 1 Introduction

The amount of radiation absorbed or reflected from sediment at any wavelength on the electromagnetic spectrum depends on its composition. In the visible light spectrum (around 400-800 nm), this difference in absorptivity and reflectivity is perceived as a difference in sediment color. For instance, minerals with low reflectivity will appear optically dark, and minerals with high overall reflectivity will appear optically bright. Similarly, minerals with higher reflectivity in longer wavelengths will appear reddish. Sediment reflectivity is determined by the average reflectivity of its constituent components. We can therefore measure sediment reflectivity in an attempt to reconstruct sediment composition, evaluate mineral assemblages, or help define distinct sedimentary facies (e.g. Debret et al., 2011; Wei et al., 2014). Reflectively-based analyses have the advantage of being rapid, non-destructive, and obtainable at a very high spatial resolution.

Several methods have been used to provide objective, user independent measurements of color for use in sedimentary and stratigraphic analysis. Quantification is necessary as color is not itself a sediment property, but rather the human perception of sediment reflectance across the visible light spectrum. The two most widely used are the Munsell color chart and CIELab L*a*b* referential (e.g. Schuttenhelm, 1989; Nagao and Nakashima, 1992; Nederbragt et al., 2006; Debret et al., 2011). Both are formulated as a cylindrical coordinate system with the vertical axis representing color lightness or intensity. The two horizontal axes represent different aspects of sediment color: 'hue' and 'chroma' in the Munsell color space and 'green–red' and 'blue-yellow' in the CIELab color space. Both color systems wrap the color space such that the long and short wavelength limits of the visible color spectrum (violet and red) are joined. These color spaces have been used to define notable sedimentary units (e.g. Ericson et al., 1961) and calibrated to evaluate the relative abundance of constituent components (e.g. Roth and Reijmer, 2005; Debret et al., 2006, 2011). These methods are, however, poorly adapted for quantitative analysis of sediment composition as the color spaces are defined for the optical perception of color instead of the underlying reflectance values (Debret et al., 2011).

Sediment reflectance spectra, which map out the sediment reflectance across the visible light spectrum, are better suited for quantitative compositional analyses or the identification of specific compounds. Raw spectra can be used, but more commonly the first derivative of the spectrum is taken with respect to wavelength, known as a first derivative spectra (Debret et al., 2011). Raw spectra have been used for evaluating the effect of differing water content (e.g. Balsam et al., 1997) while first derivative spectra peaks have been used to identify different minerals (e.g. Goethite: 445 and 525 nm, Hematite: 555-575 nm) and other compounds (e.g. chlorophyll-$\alpha$: 675 nm; Debret et al., 2011). Spectral brightness across different wavelengths can also be used as independent variables for factorial analysis, and the results interpreted in terms of one or more mineral abundances (Damuth and Balsam, 2003; Ortiz et al., 2009).

Quantitative spectrophotometric analysis of sediment composition always requires external geochemical calibration, and remains limited to detecting a small number of constituents (Debret et al., 2011). Nevertheless, changes in sediment reflectance (often measured in terms of 'color'), through its relation to underlying sediment properties, can provide a high resolution record of local climatic or environmental variability. Sediment reflectance or color has been used to reconstruct summer temperatures in South America (von Gunten et al., 2009; Elbert et al., 2015), evaluate precipitation changes from the Asian monsoon (Ji

https://doi.org/10.5194/cp-2022-29
Preprint. Discussion started: 20 April 2022


Climate of the Past Discussions

et al., 2005; Zhang et al., 2007), reveal wet-dry cyclicity in Far East Russia (Wei et al., 2014), track relative sea level changes in the tropics (Roth and Reijmer, 2005), and reconstruct patterns of oceanic sediment transport in the high northern and southern latitudes (Helmke et al., 2002; Wu et al., 2019). Existing studies highlight the wide range of environmental and climatic variables which have been reconstructed using sediment optical properties, but also that a detailed understanding of the local system is crucial for its use as a proxy (e.g. Balsam et al., 1999; Debret et al., 2011; Wei et al., 2014).

Prior literature shows that changes in sediment reflectance or color can be controlled by a wide range of climatic and environmental conditions. Here, we test two hypotheses related to the link between sediment reflectance and climate at Lago Argentino, Argentinian Patagonia. First, we hypothesize that sediment pixel intensity, and indirect measure of reflectance derived from 20 $\mu$m resolution digital core scans, can be used to reconstruct past temperature, precipitation, or wind speed changes. Secondly, we hypothesize that the correlation between sediment pixel intensity and climatic variables can provide insight into the climatic drivers of sedimentation at Lago Argentino.

## 2 Setting

Lago Argentino is the largest of several ultra-oligotrophic, ice-marginal lakes located on the eastern flank of the Southern Patagonian Icefield (SPI) at 50 °2'S, 72 °4'W (Fig. 1). Lago Argentino has a surface area of around 1500 km$^2$ and is up to 600 m deep (Sugiyama et al., 2016; Magnani et al., 2019). While precipitation is as high as several metres of water equivalent per year on the SPI itself, most of the landscape surrounding Lago Argentino is semiarid and receives less than 500 mm of precipitation per year (Garreaud et al., 2012; Lenaerts et al., 2014).

Lago Argentino is located within a tectonically and volcanically active region, and three active volcanoes are located within 100 km of the lake. Bedrock geology varies from metasedimentary and volcanic rocks in the Andean fold and thrust belt to the west of Lago Argentino, to a forearc basin sedimentary sequence and plateau basalts to the east of the fold and thrust belt (Coutand et al., 1999). Six glaciers feed into Lago Argentino, of which three (Upsala, Perito Moreno and Spegazzini) calve directly into the lake and three (Onelli, Mayo and Ameghino) calve into smaller peripheral lakes (Figure 1). Upsala glacier drains around 400 km$^3$ of ice, approximately three quarters of the ice volume in Lago Argentino's catchment (Carrivick et al., 2016; Millan et al., 2019), and calves into the longest and deepest fjord in the north-western branch of Lago Argentino. Two major rivers are located at the east of the main basin of Lago Argentino, one of which flows into the lake (Río La Leona), while the other drains the lake to the Atlantic Ocean (Río Santa Cruz).

The monthly average surface air temperature at Lago Argentino varies from a January (austral summer) maximum of around 10 °C to a July (austral winter) minimum of around -2 °C, as measured at El Calafate airport. The wind speed follows a similar cycle, with a monthly maximum of 14.2 m.s$^{-1}$ (in January) and minimum of 6.8 m.s$^{-1}$ (in June; source: El Calafate airport). Local winds are dominantly westerlies, with 70% of measured wind directions in the range 230-320 ° (SW–NW). High wind speeds keep the majority of Lago Argentino ice free even during the winter, when temperatures are below freezing. Local precipitation at El Calafate reaches a minimum of 11.5 mm/month in November, and a maximum of 28.5 mm/month in May.

https://doi.org/10.5194/cp-2022-29
Preprint. Discussion started: 20 April 2022


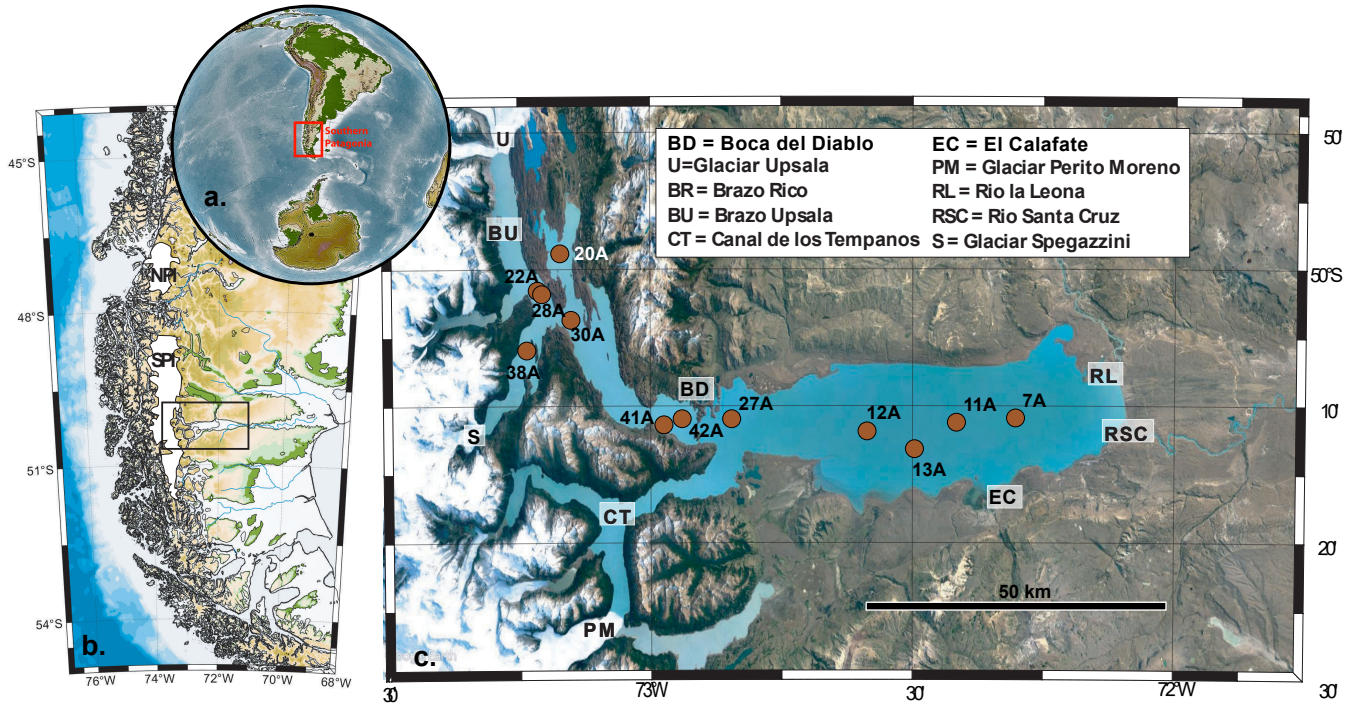


**Figure 1.** Location of Lago Argentino and other key locations. The central globe (a) shows the location of Patagonia, and the left hand panel (b) shows the location of Lago Argentino within Patagonia. The right hand panel (c) shows the position of the 10 gravity cores used in this study. Imagery © Google Earth.

The melt rates and flow velocities of the glaciers draining into Lago Argentino also vary seasonally, with a maximum in the summer (Mouginot and Rignot, 2015; Minowa et al., 2021).

## 3 Methods

### 3.1 Core collection and imaging

We collected 47 sediment cores from Lago Argentino in August–September 2019, with sediment recovery of up to 6.4 m at shallow water (<300 m depth) sites and 5.5 m at deep water (>300 m depth) sites. The total core length recovered was ~108 m. We conducted the coring in the austral winter due to lower wind speeds. We collected cores from half the locations using a Kullenberg piston-coring system with 250-450 kg head weight, and from the other half using a smaller gravity surface coring device. We identified coring sites through a preceding seismic reflection survey (Magnani et al., 2019), and collected cores from all of Lago Argentino's main depositional environments, as well as a proximal-distal transect away from the glacier fronts.

We performed initial whole-core scans of magnetic susceptibility and gamma-beam density, and split the cores lengthwise into two halves at the CSD Facility. We then conducted near-UV to near-IR spectrophotometric and magnetic scans on each

https://doi.org/10.5194/cp-2022-29
Preprint. Discussion started: 20 April 2022


Climate of the Past Discussions

split core face. We described the key sediment properties, lithological units, and sediment structures of the 47 cores in logging software PSICAT (Reed, 2007).

We selected a subset of 10 gravity cores from our whole dataset for further analysis. The subset forms a proximal-distal transect away from Glaciar Upsala, the largest glacier calving into Lago Argentino. We selected the 10 cores for their well-preserved core tops and presence of intact, alternating bright and dark laminations.

We used a Cr source ITRAX X-ray fluorescence (XRF) scanner to investigate the composition of these cores. We ran a 5 mm resolution whole-core scan on three cores from the west (ice-proximal), centre, and east (ice-distal) of Lago Argentino. We normalized XRF data for individual elements by the total counts-per-second, but did not attempt external calibration to absolute concentrations. We used a GeoTek Geoscan V line scanner to capture 20 $\mu$m resolution digital pixel intensity (PxI) core scans. We performed core scanning immediately following splitting to avoid optical property changes related to water loss or oxidation. The Geoscan V line scanner captures image data sequentially down the length of the entire core, avoiding stitching effects or spherical distortions associated with standard area-imaging cameras. We scanned each core with two focal ratios, F8 and F11, to ensure non-saturation while imaging both bright and dark sediment. The core subset used in this study is predominantly composed of bright-colored sediment, so we used the F8 focal ratio images.

### 3.2 Extraction of annual core color timeseries

Lago Argentino's sediment is predominantly composed of alternating bright and dark laminae These laminae are varves, which has been confirmed by their sedimentary structure and $^{137}$Cs dating (Van Wyk de Vries et al., 2022). Manual counting of a large number of varves is challenging to reproduce and has a limited assessment of uncertainties (Sprowl, 1993; Tian et al., 2005), we therefore used a semi-automated method to overcome these limitations. We counted the number and thickness of varves in our cores using sliding-window autocorrelation of greyscale digital core scans (CountMYvarves; see Van Wyk de Vries et al., 2021). CountMYvarves conducts multiple simultaneous lamina counts, which allows for uncertainties to be propagated into the resulting age-depth model and sedimentation rate curve.

We used the boundaries calculated from semi-automated varve counting to extract the 3-band (red, green, and blue; RGB) digital core scan image for each individual varve. We created four additional image bands, the greyscale, red/green, red/blue, and green/blue PxI (Figure 2).

### 3.3 Comparison between sediment RGB scans and XRF

We correlated sediment greyscale and RGB pixel intensities with XRF results to investigate the relationship between digital core scan color and sediment elemental composition. We extracted the mean pixel intensities for the seven image bands at the same location as each XRF measurement, averaging a 5 mm wide band across-core and the XRF measurement resolution down-core. We repeat this process for each of the three cores analysed. We then calculated a correlation matrix between the down-core variation in 8 elements measured by the ITRAX XRF scanner (Si, Al, K, Ca, Fe, Ti, Rb and Sr) and the four mean PxIs (greyscale, red, green, and blue) and three PxI ratios (red/green, red/blue, and green/blue). The correlation coefficient ($r$-value) between any two variables $A$ and $B$ is calculated as:

https://doi.org/10.5194/cp-2022-29
Preprint. Discussion started: 20 April 2022


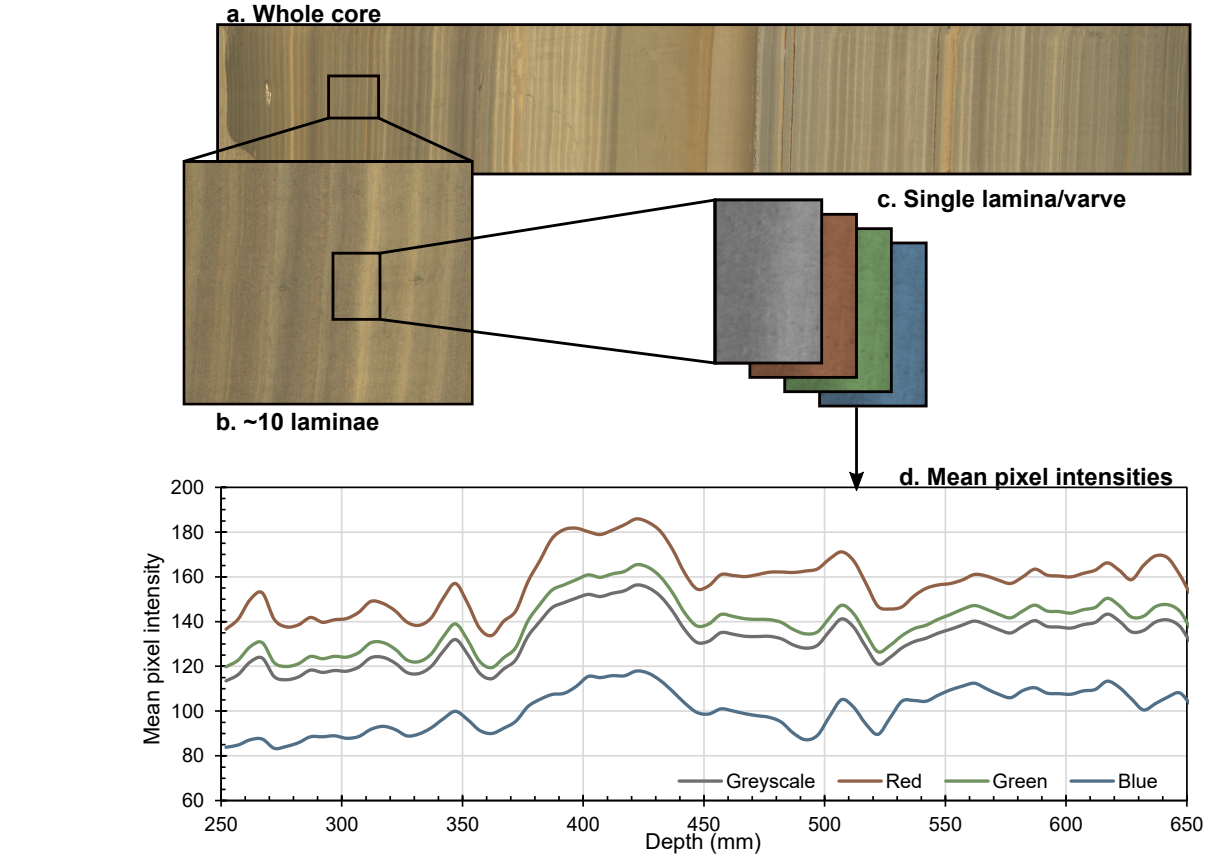


**Figure 2.** Extraction of color depth-series from raw digital core scans. (a) and (b) show a whole core scan and ∼10 laminae scan subsection. (c) shows a single varve split out into the four different bands, and (d) shows the whole-core PxI depth-series for each band.

$$r(A,B) = \frac{1}{N-1}\sum_{i=1}^{N}\left(\frac{A_i-\mu_A}{\sigma_A}\right)\left(\frac{B_i-\mu_B}{\sigma_B}\right), \tag{1}$$

with $N$ being the size of each sample, $\mu_A$ and $\mu_A$ being the averages of each variable, and $\sigma_A$ and $\sigma_A$ being their standard deviations. Due to the risk of false correlations, we calculate a new significance threshold $Sig$ by dividing the threshold for 95% statistical significance by the number of pairwise correlations computed $n$:

$$Sig = \frac{0.05}{n} = \frac{0.05}{8*9} = 0.0009. \tag{2}$$

We calculated a corresponding correlation $p$-value matrix, and considered correlations with $p$-values lower than 0.0009 to be significant.

https://doi.org/10.5194/cp-2022-29
Preprint. Discussion started: 20 April 2022


Climate of the Past Discussions

### 3.4 Correlation between sediment pixel intensities and climatic variables

We evaluated the correlation between sediment PxIs and three climatic variables: precipitation, temperature, and wind speed. We accounted for two separate temporal uncertainties in our age-depth model: possible missing time from disrupted varves at the sediment-water interface (i.e the first identifiable varve might not correspond to 2019, the year the cores were collected), and uncertainties from varve counting. We computed 1000 possible age-depth models for each core using Monte Carlo sampling of the uncertainty derived from the semi-automated varve counting and plausible numbers of missing varves at the sediment-water interface.

We obtained temperature and precipitation covering the period 1930-2020 from the CRU-TS 4.05 monthly time series for the half-degree grid cell centered on 50.25°S, 72.75°W (Harris et al., 2020). This dataset combines records from several meteorological stations around Lago Argentino (e.g. Ibarzabal Y Donangelo et al., 1996) into a single homogeneous record. We obtained daily wind speed data from El Calafate airport covering the period 1963-2017. We resampled the precipitation, temperature, and wind records into three separate time series: a mean annual record, a mean austral summer December-January-February (DJF) record and a mean austral winter June-July-August (JJA) record. We used equation (2) to perform a cross-correlation between individual PxI time series and climate time series. We calculated a correlation coefficient for each individual PxI timeseries of the 1000 age-depth model ensemble.

## 4 Results

### 4.1 Compositional significance of pixel intensities

In ice-distal core 7A, greyscale, green, and blue PxIs show little to no correlation with XRF-derived sediment composition. Red PxI shows a strong positive correlation with Al, Ti, Fe, and Rb ($r$-value $> 0.35$), a weaker positive correlation with K, and a strong anticorrelation with Ca, Si, and Sr ($r$-value$<$-0.35). The red/green, red/blue, and green/blue PxIs show strong positive correlations with Si, Ca, and Sr, a weaker positive correlation with K, and a strong anticorrelation with Al, Ti and Fe (Figure 3).

In core 27A, from the western margin of the main lake basin, greyscale PxI shows a weak anticorrelation with all elements. Blue PxI exhibits no strong correlation with any element. Red PxI shows a strong positive correlation with Al, Si, Ti, Ca, and Fe ($r$-value $> 0.35$) and a weak positive correlation with all other elements (Figure 3). Green PxI shows a strong positive correlation with Sr, a weak positive correlation with Ca, a strong anticorrelation with K, and a weak anticorrelation with other elements. All band ratio PxIs are strongly anticorrelated with Al, K, Ti, and Fe ($r$-value$<$-0.35). The Green/blue PxI is also strongly correlated with Ca and Sr ($r$-value $> 0.35$).

In ice-proximal core 28A, blue PxI shows little to no correlation with any element. Greyscale PxI and all three band ratio PxIs are very strongly anticorrelated with Al, Si, K, Ca, Ti, and Fe ($r$-value$<$-0.7). The green PxI exhibits the same correlations to a slightly lesser degree ($r$-value of 0.5). The red PxI shows the opposite pattern, with a very strong positive correlation with Al, Si, K, Ca, Ti, and Fe ($r$-value $> 0.8$). Greyscale, green, red/green, and red/blue PxIs show a strong correlation with Sr

https://doi.org/10.5194/cp-2022-29
Preprint. Discussion started: 20 April 2022


Climate of the Past Discussions
Open Access
EGU

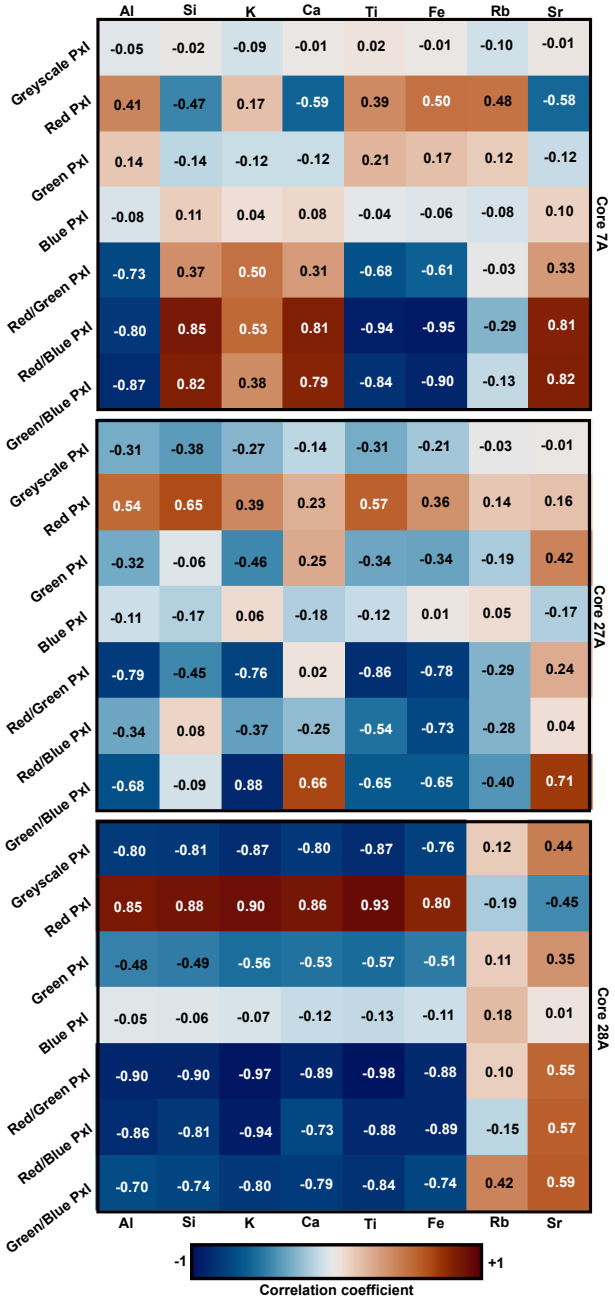


**Figure 3.** Correlations between the four PxI depth-series and selected elements from the XRF scanner.

170 ($r$-value $>$ 0.35), while the red PxI shows a strong anticorrelation with Sr ($r$-value$<$-0.35), and the green/blue PxI shows a strong correlation with both Rb and Sr ($r$-value $>$ 0.35).

https://doi.org/10.5194/cp-2022-29
Preprint. Discussion started: 20 April 2022


Climate of the Past Discussions

Overall, the ice-proximal core PxI shows a strong (positive or negative) correlation with all major elements studied. The two cores from western and eastern margins of the main lake basin exhibit more complex patterns, with an overall positive correlation between the red PxI and Al, Ti, K, Fe, and Rb. In addition, all three band ratios PxIs are strongly anticorrelated with Al, Ti, and Fe (Figure 3). The green/blue ratio PxI exhibits a strong positive correlation with Ca and Sr in both cores. The two cores also exhibit notable differences, with Si being strongly anticorrelated with red PxI in the eastern main lake basin (core 7A) and positively correlated to the west (core 27A). Similarly, Si is strongly correlated with red/blue and green/blue PxIs in core 7A, but shows no correlation with these PxIs for core 27A. Ca and Sr and both strongly anticorrelated with red PxI for core 7A, but are weakly correlated with red PxI for core 27A.

## 4.2 Correlation with climatic variables

We use the correlations between sediment PxI and XRF compositional data to narrow our analysis down to the most informative PxI bands: red, red/green, red/blue, and green/blue PxIs.

### 4.2.1 Temperature

Mean annual temperature is anticorrelated with red PxI in the three most ice-proximal cores (22A, 30A, 38A; 30-70% of $p$-values $<0.05$) and the westernmost core in the main lake basin (27A; 35% of $p$-values $<0.05$). All three band ratio PxIs are anticorrelated with mean annual temperature in the main lake basin, with 60-70% of $p$-values $<0.05$ for the easternmost core 11A (Figure 4). JJA temperatures exhibit a weak positive correlation with red PxI in the main lake basin, and no correlation with red PxI in the brazos (ice-proximal fjords) or with the band ratio PxIs in any part of the lake. DJF temperatures are anticorrelated with red PxI in the three most ice-proximal cores (22A, 30A, 38A; 30-75% of $p$-values $<0.05$) and westernmost core in the main lake basin (27A; 60% of $p$-values $<0.05$). Band ratio PxIs show a weak positive correlation with DJF temperature in the brazos, and a strong anticorrelation with DJF temperature in the main lake basin (30-40% and 80-85% of $p$-values $<0.05$ for cores 12A and 11A respectively).

Overall, temperature is most correlated, whether positively or negatively, with sediment PxI in the summer (Figure 4). Red and all three band ratio PxIs show different signals, with red PxI most anticorrelated with temperature in the most ice-proximal cores and western margin of the main lake basin, and band ratio PxIs most anticorrelated with temperature in the centre and east of the main lake basin.

### 4.2.2 Precipitation

Mean annual, austral winter (JJA), and austral summer (DJF) precipitation show very little or no correlation with red or band ratio PxIs in any region of Lago Argentino, with no correlation having more than 40% of significant values. Only the easternmost core 11A, red, red/green, red/blue, and green/blue PxIs exhibit a weak positive correlation with precipitation, having 25-40% of significant positive correlations with DJF precipitation (Figure 5).

https://doi.org/10.5194/cp-2022-29
Preprint. Discussion started: 20 April 2022


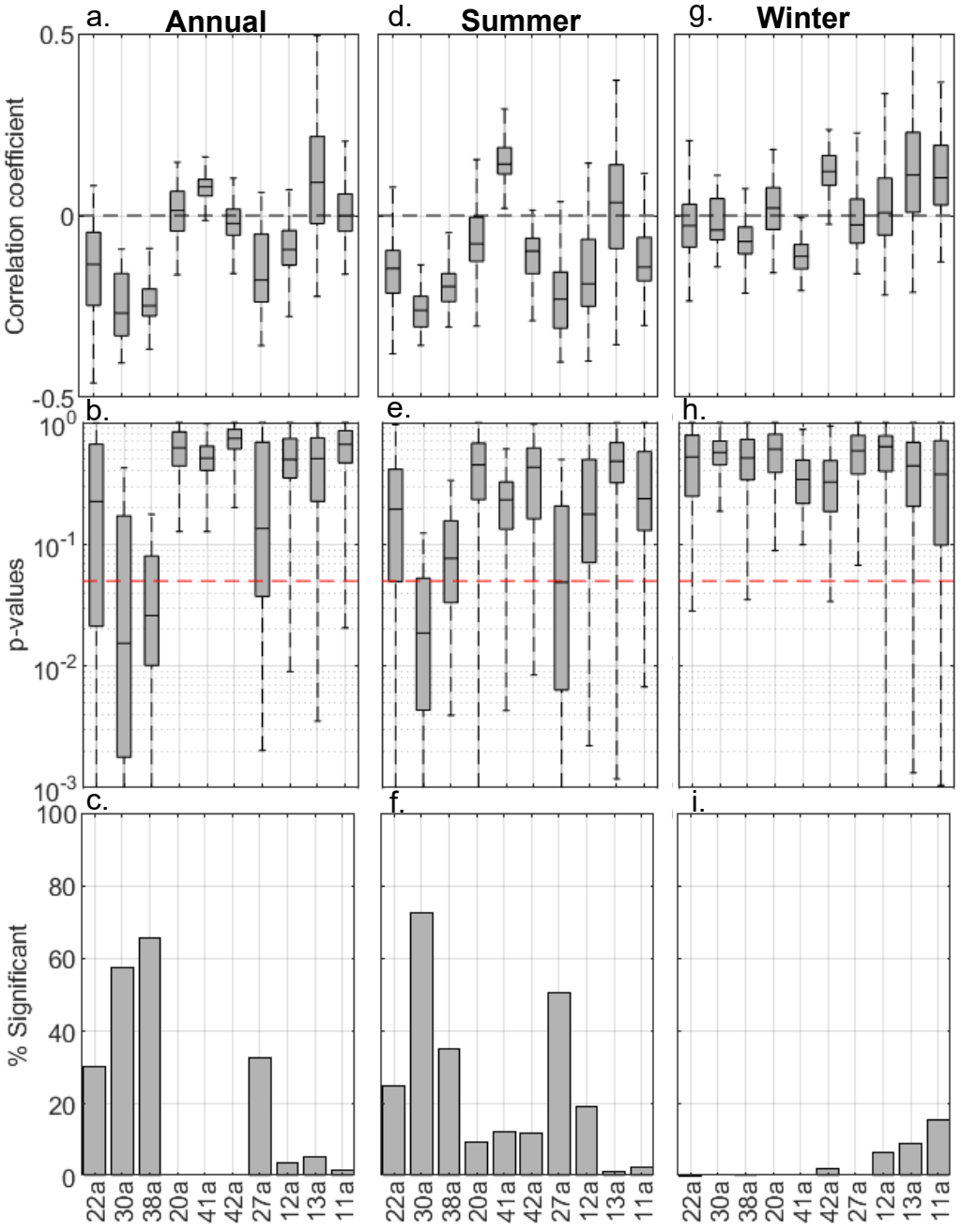


**Figure 4.** Box plot of correlation coefficients ($r$-values; a, d, g), $p$-values (b, e, h), and bar plot of percentage of correlations significant at 95% level (c, f, i) for the correlation between red PxI and annual, austral summer (DJF), and austral winter (JJA) temperatures.

https://doi.org/10.5194/cp-2022-29
Preprint. Discussion started: 20 April 2022


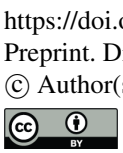

Climate of the Past
Discussions
Open Access
EGU

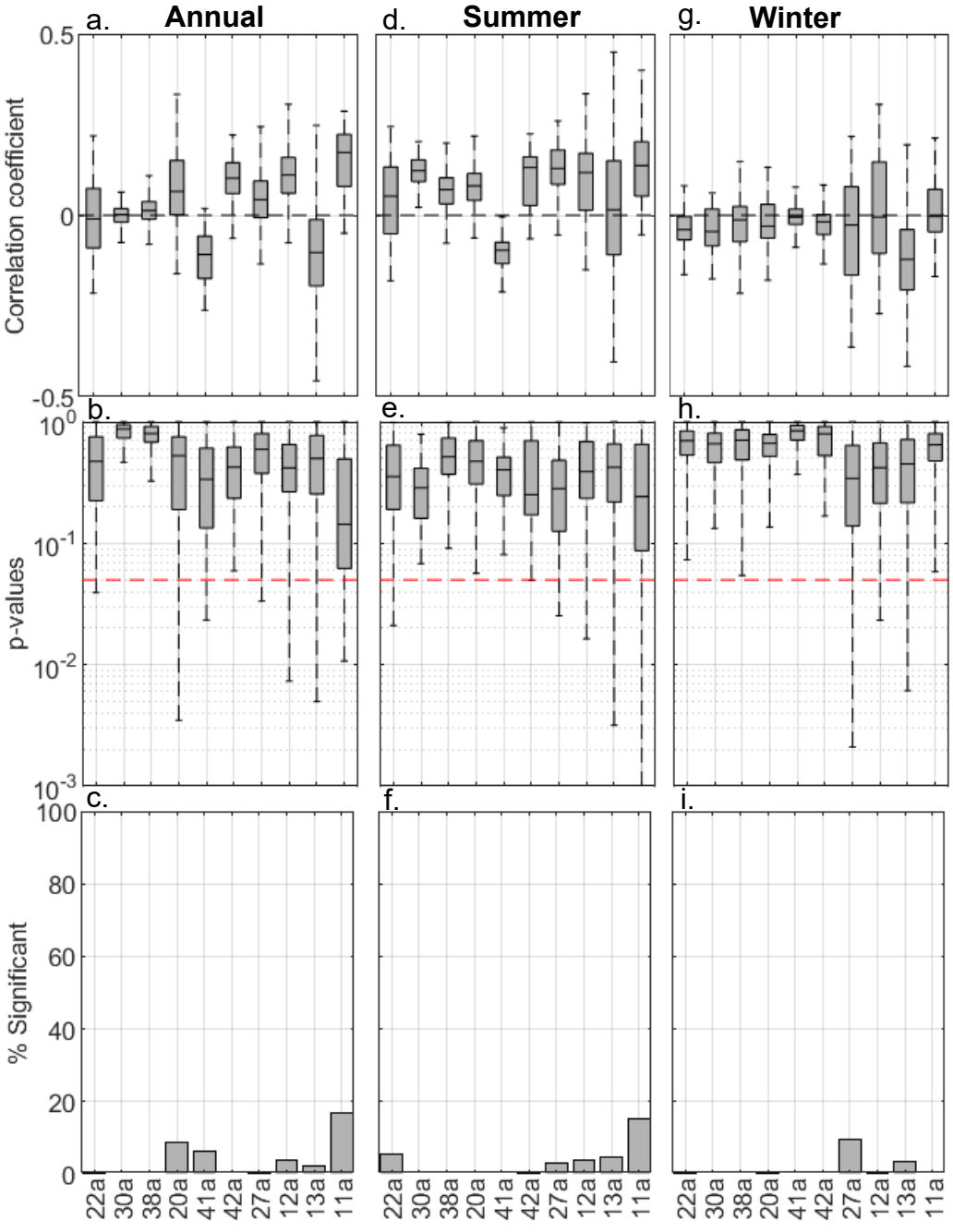


**Figure 5.** Box plot of correlation coefficients ($r$-values; a, d, g), $p$-values (b, e, h), and bar plot of percentage of correlations significant at 95% level (c, f, i) for the correlation between red PxI and annual, austral summer (DJF), and austral winter (JJA) precipitation.

https://doi.org/10.5194/cp-2022-29
Preprint. Discussion started: 20 April 2022


Climate of the Past Discussions

#### 4.2.3 Wind speed

DJF and mean annual wind speed are strongly negatively correlated with red and band ratio PxIs in the brazos (60-90% of $p$-values <0.05) and positively correlated with band ratio PxIs at the western margin of the main lake basin (core 27A; 20-40% of $p$-values <0.05). DJF wind speed is also strongly positively correlated with red PxI in easternmost core 11A ( 90% of $p$-values<0.05). In brazos cores 30A and 38A, JJA wind speed shows a similar overall pattern with weaker correlations, exhibiting a moderate anticorrelation with red PxI (15-40% of $p$-values <0.05 respectively; Figure 6). JJA wind speeds show no correlation with sediment PxI in the main lake basin. All band ratio PxIs are strongly negatively correlated with wind speed for most ice-proximal core 22A (60-95% of $p$-values <0.05) and positively correlated with wind speed in the western margin of the main lake basin (core 27A; 35-55% of $p$-values <0.05).

JJA and mean annual wind speed are most correlated with sediment PxI (Figure 6). Red PxI and band ratio PxIs show different signals, with red PxI most negatively correlated with wind speed in the most ice-proximal cores and positively correlated with wind speed in the eastern margin of the main lake basin, and band ratio PxIs most anticorrelated with wind speed at the most ice-proximal location and western margin of the main lake basin.

## 5 Discussion

### 5.1 Correlation between PxI, elemental composition, and climate

Sediment PxI exhibits significant correlations with both XRF-derived compositional data and climatic variables, linking changes in core composition to changes in temperature and/or wind speed. In this section, we first discuss and interpret the compositional significance of PxI, and the relationship between PxI, climatic variables, and sediment transport. In the second section, we discuss the advantages and disadvantages of using PxI as a paleoclimatic or paleoenvironmental proxy in Lago Argentino and more broadly through our two hypotheses: 1) that sediment pixel intensity can be used as a proxy to reconstruct past climatic changes, and 2) that the correlation between sediment PxI and climatic variables might help elucidate the details of lacustrine sedimentation.

We use the correlation between PxI and XRF data to evaluate the compositional significance of core PxI in Lago Argentino's different depositional environments. Ice proximal core 28A shows a strong positive correlation between red PxI and all major elements (Al, Si, K, Ca, Fe), as well as a strong anticorrelation between green PxI, band ratio PxIs and major elements. Possible minerals enriched in these elements include various feldspars, pyroxenes, and clays which more strongly reflect long wavelength red light, and weakly reflect shorter wavelength green light. Core 27A from the western main lake basin shows a strong positive correlation between red PxI and Si, Al, Ti, K, and Fe, and the weakest correlation for Ca, Sr, and Rb. Possible minerals enriched in these elements include quartz, K-feldspar, various pyroxenes, ilmenite and other phases. Fe-rich minerals often appear optically red. Core 7A from the eastern margin of the main lake basin exhibits a strong correlation between red PxI and Al, Ti, K, Fe, and Rb, and a strong anticorrelation with Si, Ca, and Sr. This suggests a similar mineral assemblage to the western margin of the main lake basin, but with the optically red phases more depleted in silicon. This could be caused

https://doi.org/10.5194/cp-2022-29
Preprint. Discussion started: 20 April 2022


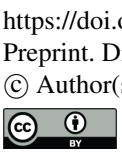

Climate of the Past Discussions
Open Access
EGU

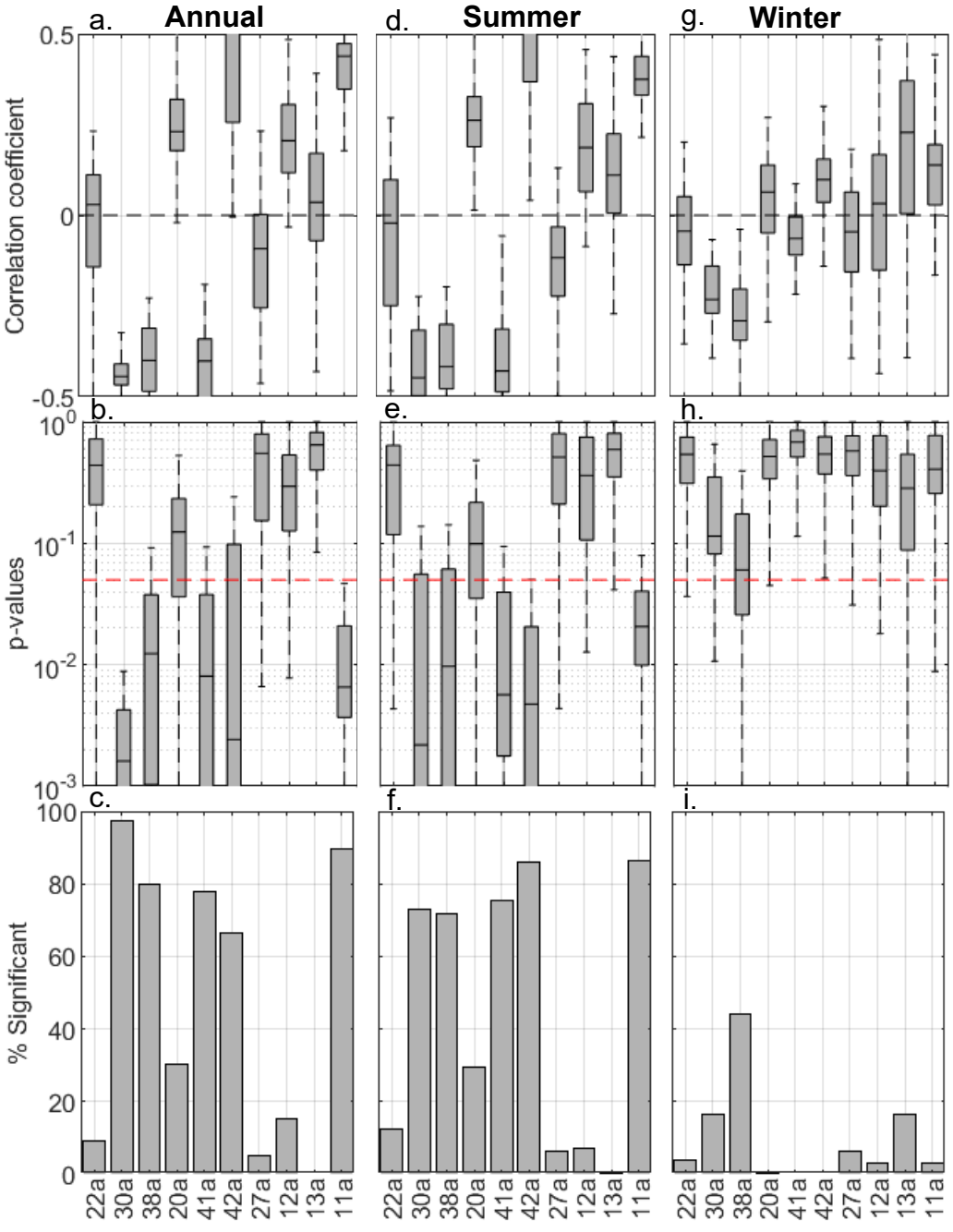


**Figure 6.** Box plot of correlation coefficients ($r$-values; a, d, g), $p$-values (b, e, h), and bar plot of percentage of correlations significant at 95% level (c, f, i) for the correlation between red PxI and annual, austral summer (DJF), and austral winter (JJA) wind speeds.

https://doi.org/10.5194/cp-2022-29
Preprint. Discussion started: 20 April 2022


Climate of the Past Discussions

by a greater proportion of non-silicate minerals, such as ilmenite or haematite. Analysis of lamina-scale stratigraphy in Lago Argentino (Van Wyk de Vries et al., 2022) reveals distinct characteristics between the bright and dark layers:

- Optically bright, winter layers have a relatively low Ca/K ratio and a finer grain size distribution
- Optically dark, summer layers have a higher Ca/K ratio and a coarser grain size distribution.

Similarly, our results show a strong positive correlation between sediment red band PxI and K and a weak correlation or anticorrelation between red band PxI and Ca.

We evaluate the possible climatic controls on sediment production, transport, and preservation to contextualize the relationship between PxI and climatic variables. We separate sediment production, transport, and preservation, as each affects the quantity and type of sediment recorded in a lake in different ways. At Lago Argentino, sediment is primarily produced through glacial erosion, with a minor contribution from fluvial erosion (Van Wyk de Vries et al., 2022). At a first order, glacial erosion rate is controlled by basal sliding speed, which is in turn related to the subglacial water pressure (Cuffey and Paterson, 2010; Cook et al., 2020). Temperature can therefore influence glacial erosion by affecting surface melting and the quantity of water at the glacier bed. The magnitude of this effect is, however, challenging to quantify as the relationship between water production, glacier sliding velocity, and glacial erosion are complex (Cuffey and Paterson, 2010; Cook et al., 2020).

Sediment transport occurs primarily through the movement of suspended sediment particles through Lago Argentino, with a lesser contribution from subglacial and fluvial sediment transport. Subglacial sediment transport is high when abundant meltwater reaches the glacier bed and the subglacial drainage system is channelized (related to glacier bed dynamics). Fluvial sediment transport is high when river discharge is high, related to high precipitation or rapid ice melt in the case of proglacial rivers. Lacustrine sediment transport is related to water circulation within the lake, the degree of mixing of the water, and the settling velocity of individual particles (Fischer et al., 1979; Spigel and Imberger, 1980; Imberger and Patterson, 1989; Sugiyama et al., 2016). Lake geometry and bathymetry also affect sediment transport, with constrictions such as Boca del Diablo (Figure 1) inhibiting sediment through-flow. Lacustrine sediment transport might therefore be affected by wind induced surface currents, seiches, and deeper circulation cells (Imberger and Patterson, 1989; Tylmann et al., 2013; Richter et al., 2016) and temperature induced lake stratification (Lewis, 1983; Imberger and Patterson, 1989). Sediment can also be temporarily rafted in icebergs. Iceberg production rate is related to glacier calving rate, while iceberg motion through the lake is driven by surface winds and subsurface currents.

Finally, sediment quantity and type can be influenced by the resuspension, erosion, or reworking of previously deposited sediment. Lago Argentino is an ultra-oligotrophic lake, with very few traces of bioturbation in any of the cores studied. Sediment can be resuspended at a lake bed from strong wind-induced currents (Kristensen et al., 1992; Bailey and Hamilton, 1997; Carper and Bachmann, 2011), although this process is limited to lakes at most a few tens of metres deep. The shallowest core analysed in this study was collected at a water depth of 99 m, and the deepest at a water depth of 464 m; all well below the wave base (Bengtsson et al., 2012). Any sediment deposited in Lago Argentino is therefore preserved in the sedimentary record.

https://doi.org/10.5194/cp-2022-29
Preprint. Discussion started: 20 April 2022


Climate of the Past Discussions

Temperature exhibits a strong correlative relationship with various sediment PxIs in the summer, but little to no correlation in the winter. Wind speed exhibits a strong correlation with sediment PxI in the summer, and a moderate to weak relationship during the winter. Precipitation exhibits little correlation with sediment PxI at any time of year.

Temperature can influence both sediment production and sediment transport at Lago Argentino. We expect the strongest correlative relationship between temperature and sediment PxI in different locations depending on the mechanism by which temperature affects sedimentation. If it affects sedimentation through changes in glacier surface melting, erosion, and subglacial sediment transport, we expect the strongest correlative relationship close to the glacier fronts. Conversely, if temperature affects sedimentation through changes in lake-water stratification, we expect the strongest correlative relationship to be distributed through the main lake basin. Our results show high correlations in both of these zones: DJF temperature shows a strong anticorrelation with red PxI in the ice-proximal cores 22A, 30A, and 38A and a strong anticorrelation with band ratio PxIs in main lake basin cores 11A and 12A. At Lago Argentino, wind speed does not affect sediment production or resuspension, but might affect sediment transport. Both red and band ratio PxIs are strongly anticorrelated with DJF wind speed in the ice proximal brazos. Red PxI is positively correlated with DJF wind speed in the main lake basin, while band ratios are weakly anticorrelated or show no relationship. The inverse relationship between the ice-proximal and ice-distal regions of Lago Argentino suggests that higher than average winds promote distal-to-proximal lacustrine circulation and transport sediment from ice-proximal towards ice-distal regions of the lake.

### 5.2 PxI as a paleoclimatic proxy

Sediment PxI is significantly correlated with summer temperature and wind speed in multiple cores. In this section, we explore whether the relationship between PxI and temperature or wind speed might be used as a paleoclimatic proxy to reconstruct past climatic conditions beyond the observational period. For PxI to be useful as a paleoclimatic or paleoenvironmental proxy, we must be able to use its relationship with the modern instrumental period to calibrate a predictive model and reconstruct temperature over the period pre-dating instrumental measurements (Gornitz, 2009; McShane and Wyner, 2011; Tingley et al., 2012). PxI's ensemble median correlations meet the $p$-value$<$0.1 significance threshold for inclusion as a proxy, as defined by Mann et al. (2008). For summer air temperature, this correlation significance threshold is met by 3 cores (out of 10) for red PxI, 2 cores for red/green and red/blue PxIs, and 4 cores for green/blue PxI. For summer wind speed, this correlation significance threshold is reached by 6 cores for red PxI, 3 cores for red/green PxI, and 1 core for red/blue and green/blue PxIs. No core reaches this significance threshold for precipitation. Based on this correlation significance alone, we might conclude that PxI is a suitable paleo-temperature and paleo-wind speed proxy in multiple cores.

A significant correlation between proxy and climatic data is, however, not sufficient for a proxy to have hindcasting value beyond the calibration time-period. For the standard linear regression approach to proxy reconstruction, two additional assumptions must be made: linearity and stationarity (National Research Council, 2006). Linearity refers to the statistical relationship between a given proxy and the climatic variable it is calibrated to, which must approach a first-order polynomial. Stationarity, similar to Lyell's "uniformity principle" (Lyell, 1830; Camardi, 1999) refers to the assumption that the statistical relationship between a given proxy and a given climatic variable remains constant throughout the entire period of interest (National Re-

https://doi.org/10.5194/cp-2022-29
Preprint. Discussion started: 20 April 2022


Climate of the Past Discussions

search Council, 2006). In practice, the relationship between the proxy and climatic variable (leading to the correlation) must exhibit only small changes through time, or else the predictive power of the proxy will be lost and any reconstructions will be meaningless. In an extreme scenario, environmental changes could cause the relationship between proxy and climatic variable to become inverted through time, leading to the proxy predicting the opposite paleoclimate to reality. We focus on whether the second assumption (stationarity) is met at Lago Argentino, which exhibits strong spatial variability and a non-unique relationship between the proxy and climatic variables of interest.

The strong spatial variability in Lago Argentino is best illustrated by the correlation between DJF wind speed and red PxI in cores 41A and 42A, located within 3 km of each other in a region where the lake is at its narrowest. Both cores' red PxI exhibit highly significant ($p$-values$<$0.01) correlations with DJF wind speed, but with opposing signs: a strong negative correlation at core 41A (median $r$-value of -0.45) and a strong positive correlation at core 42A (median $r$-value of 0.5). With opposing relationships to climatic drivers within a 3 km length-scale (for a 100 km long lake), even a small spatial shift in sedimentation patterns across Lago Argentino would strongly affect the relationship between sediment PxI and climate at any given location. Any down-core shift in the relationship between sediment PxI and climate would contradict the assumption of stationarity.

The relationship between PxI and climatic variables is also non-unique, as our data shows a statistically significant relationship with both temperature and wind speed. Summer temperature and wind speed themselves do not co-vary ($r$-value = 0.06; $p$-value = 0.67), and therefore cannot both be accurately reconstructed using a single proxy. Furthermore, if the contribution of temperature and wind speed has not remained steady through time, PxI might record these climatic drivers to different degrees through time. For instance, the effect of wind could have dominated over temperature during periods when the mean temperature at Lago Argentino was colder than present. Such a case would also invalidate the assumption of stationarity. We cannot assess the relative effect of temperature and wind speed on PxI beyond the instrumental period, which limits the potential of PxI to predict paleo-temperatures and paleo-wind speeds.

PxI is not significantly related to precipitation at Lago Argentino, so cannot be used as a paleo-precipitation proxy. The use of PxI as a paleo-temperature or paleo-wind speed appears statistically plausible based on its correlation with climatic variables, but the non-uniqueness and strong spatial variability of this relationship suggest that stationarity cannot be assumed at Lago Argentino. We therefore conclude that PxI is also not a suitable proxy for temperature or wind speed.

While it is not a suitable proxy for any climatic variable, correlation (or lack thereof) between sediment PxI and temperature, precipitation, and wind speed does reveal differing controls on sedimentation in the summer and winter, and across Lago Argentino. Mean annual, DJF, and JJA precipitation show no relationship with PxI, showing that precipitation does not exert a systematic control on sedimentation within Lago Argentino. Mean annual and DJF temperature and wind speed are both correlated with red and band ratio PxIs. Overall, DJF temperature anticorrelates with red PxI across the entire basin, while DJF wind speed is anticorrelated in the ice proximal brazos and correlated in the ice-distal main lake basin. JJA temperature shows no relationship with PxI, while JJA wind speed is weakly anticorrelated in the ice proximal brazos and correlated in the ice-distal main lake basin.

In the summer, an influx of optically dark sediment is enhanced close to the glacier fronts by high temperatures, or suppressed by low temperatures. In the main basin of the lake, settling of these same optically dark grains is promoted during times of

https://doi.org/10.5194/cp-2022-29
Preprint. Discussion started: 20 April 2022


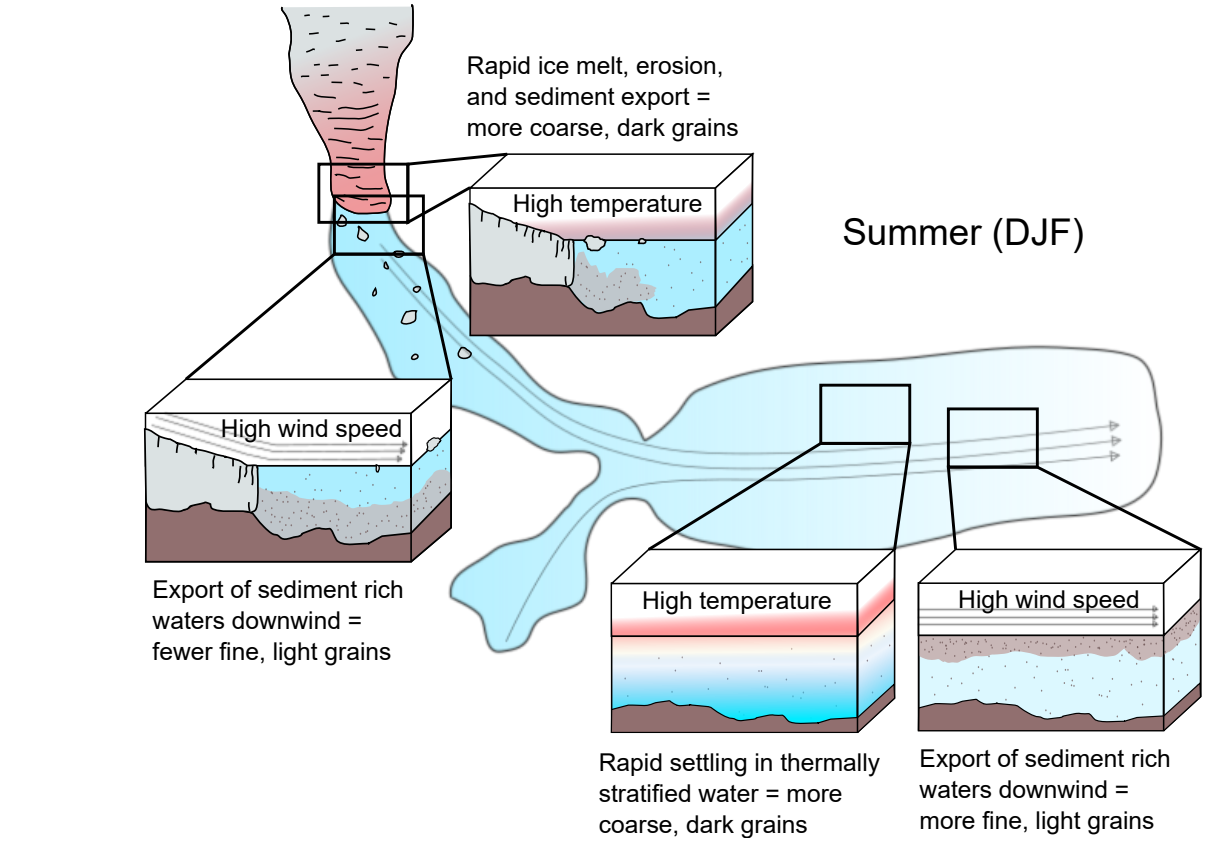


**Figure 7.** Summary diagram of key climatic controls on sedimentation in Lago Argentino in the austral summer (DJF).

high temperature by a strong thermal stratification and limited vertical water column mixing, while low temperatures suppress this stratification (Figure 7). In addition, higher than average summer wind speeds drive enhanced horizontal mixing and increased migration of sediment-rich waters towards ice-distal regions of the lake, thus reducing settling of optically bright grains close to the ice front and increasing it in the main lake basin. The effect of higher than average wind speeds is also present in the winter, although to a lesser extent. Detailed, basin-wide measurements of lake circulation and suspended sediment concentrations (Sugiyama et al., 2016, 2021) yield similar information about the drivers of sedimentation across the lake basin. Such measurements are, however, expensive and logistically challenging to collect, and are available at few locations. We show here that correlation between sediment properties and local climatic variables can yield similar information about the large-scale climatic drivers of sedimentation.

https://doi.org/10.5194/cp-2022-29
Preprint. Discussion started: 20 April 2022



## 6 Conclusions

We evaluated whether the optical properties of a large dataset of cores from Lago Argentino, southern Patagonia, provide a suitable paleoclimate proxy, and what they show about the dominant climatic drivers of sedimentation. We used 20 micron resolution linescan images and semi-automated varve counts to extract annual resolution sediment pixel intensity data. We then compared this pixel intensity data to both x-ray fluorescence compositional data of these same lake cores, and local temperature, precipitation, and wind speed data. We showed that sediment pixel intensities are significantly correlated with XRF compositional data, with red, red to green ratio, red to blue ratio, and green to blue ratio pixel intensities exhibiting the strongest relationship with available major elements. Pixel intensities have significant correlations with austral summer (DJF) temperatures and wind speeds, but not with precipitation. We established that several cores reach the correlation significance thresholds for use as paleo-temperature or paleo-wind speed proxies, but that the assumption of stationarity cannot be made at Lago Argentino. Despite being unsuitable as paleoclimatic proxies, our data reveals how climate affects sedimentation in this location: 1) precipitation does not affect sedimentation; 2) high summer temperatures promote ice melt and thermal stratification, increasing the settling of coarser, optically dark grains; 3) high wind speeds, particularly in the summer, increase the lateral flux of sediment-laden waters from ice-proximal to ice-distal regions of Lago Argentino, decreasing the settling of optically bright, fine grains in the brazos and increasing it in the main lake basin. Our data highlights that caution must be applied when searching for paleoenvironmental proxies in complex environments, and that records unsuitable for use as proxies might still yield valuable information about their sedimentary environment.

*Data availability.* Full resolution core scans and stratigraphic information are available at 10.5281/zenodo.5815107. The code used to count laminations in the cores, countMYvarves is freely available under a GPL3.0 license at doi.org/10.5281/zenodo.4031812.

*Author contributions.* MV conceived the study. All authors conducted the lake coring and/or processed the cores in the CSD Facility laboratory. MV processed the data, all authors interpreted the data and edited the manuscript.

*Competing interests.* The authors declare no competing interests.

*Acknowledgements.* MV was supported by a University of Minnesota College of Science and Engineering Fellowship and a Doctoral Dissertation Fellowship. We acknowledge the critical role played by logistical and design expertise of Ryan O'Grady and Anders Noren of the CSD Facility in planning and field phases of this research. Kristina Brady Shannon, Jessica Heck, Alex Stone and Rob Brown seamlessly coordinated core processing and analytical activities at the CSD Facility. We thank Anastasia Fedotova, Cristina San Martín, Guillermo Tamburini-Beliveau, Alexander Schmies and Shanti Penprase for their help with core recovery and processing, and all Spanish-speaking

https://doi.org/10.5194/cp-2022-29
Preprint. Discussion started: 20 April 2022


team members for their critical contribution of language skills. Pedro Skvarca, Scientific Director of the Glaciarium Interpretive Center, provided important planning and logistical assistance during initial phases of work. We particularly thank Capitán Alejandro Jaimes for his expert handling of the MV Janet, and for sharing his incisive knowledge of Lago Argentino. We also acknowledge Robert Brown from the University of Minnesota Duluth for acquiring the XRF data. This material is based upon work supported by the National Science Foundation under Grant No. EAR-1714614, coordinated by Lead PI Maria Beatrice Magnani. Data on the LArg cores are available from the CSD Facility at https://cse.umn.edu/csd/projects. Full resolution core scans and stratigraphic information are available at 10.5281/zenodo.5815107. The code used to count laminations in the cores, countMYvarves, is freely available under a GPL3.0 license at doi.org/10.5281/zenodo.4031812.

https://doi.org/10.5194/cp-2022-29
Preprint. Discussion started: 20 April 2022


Climate of the Past Discussions

## References

Bailey, M. C. and Hamilton, D. P.: Wind induced sediment resuspension: a lake-wide model, Ecological Modelling, 99, 217–228, https://doi.org/10.1016/S0304-3800(97)01955-8, 1997.

Balsam, W. L., Damuth, J. E., and Schneider, R. R.: Comparison of shipboard vs shorebased spectral data from Amazon Fan cores: implications for interpreting sediment composition., in: Proceedings of the Ocean Drilling Program, Scientific Results, vol. 155, pp. 193–215, 1997.

Balsam, W. L., Deaton, B. C., and Damuth, J. E.: Evaluating optical lightness as a proxy for carbonate content in marine sediment cores, Marine Geology, 161, 141–153, https://doi.org/10.1016/S0025-3227(99)00037-7, 1999.

Bengtsson, L., Herschy, R. W., and Fairbridge, R. W.: Encyclopedia of Lakes and Reservoirs, Encyclopedia of Lakes and Reservoirs, by L. Bengtsson, R.W. Herschy, and R.W. Fairbridge. Encyclopedia of Earth Sciences Series, ISBN 978-1-4020-5616-1. Berlin: Springer Verlag, 2012, http://adsabs.harvard.edu/abs/2012elr..book.....B, 2012.

Camardi, G.: Charles Lyell and the Uniformity Principle, Biology and Philosophy, 14, 537–560, https://doi.org/10.1023/A:1006504910017, 1999.

Carper, G. L. and Bachmann, R. W.: Wind Resuspension of Sediments in a Prairie Lake, Canadian Journal of Fisheries and Aquatic Sciences, https://doi.org/10.1139/f84-217, publisher: NRC Research Press Ottawa, Canada, 2011.

Carrivick, J. L., Davies, B. J., James, W. H., Quincey, D. J., and Glasser, N. F.: Distributed ice thickness and glacier volume in southern South America, Global and Planetary Change, 146, 122–132, https://doi.org/10.1016/j.gloplacha.2016.09.010, 2016.

Cook, S. J., Swift, D. A., Kirkbride, M. P., Knight, P. G., and Waller, R. I.: The empirical basis for modelling glacial erosion rates, Nature Communications, 11, 759, https://doi.org/10.1038/s41467-020-14583-8, number: 1 Publisher: Nature Publishing Group, 2020.

Coutand, I., Diraison, M., Cobbold, P. R., Gapais, D., Rossello, E. A., and Miller, M.: Structure and kinematics of a foothills transect, Lago Viedma, southern Andes (49°30′S), Journal of South American Earth Sciences, 12, 1–15, https://doi.org/10.1016/S0895-9811(99)00002-4, 1999.

Cuffey, K. M. and Paterson, W. S. B.: The Physics of Glaciers, Academic Press, google-Books-ID: Jca2v1u1EKEC, 2010.

Damuth, J. E. and Balsam, W. L.: Data report: Spectral data from Sites 1165 and 1167 including the HiRISC section from Hole 1165B, in: Proceedings of the Ocean Drilling Program, Scientific Results, vol. 188, 2003.

Debret, M., Desmet, M., Balsam, W., Copard, Y., Francus, P., and Laj, C.: Spectrophotometer analysis of Holocene sediments from an anoxic fjord: Saanich Inlet, British Columbia, Canada, Marine Geology, 229, 15–28, https://doi.org/10.1016/j.margeo.2006.01.005, 2006.

Debret, M., Sebag, D., Desmet, M., Balsam, W., Copard, Y., Mourier, B., Susperrigui, A. S., Arnaud, F., Bentaleb, I., Chapron, E., Lallier-Vergès, E., and Winiarski, T.: Spectrocolorimetric interpretation of sedimentary dynamics: The new "Q7/4 diagram", Earth-Science Reviews, 109, 1–19, https://doi.org/10.1016/j.earscirev.2011.07.002, 2011.

Elbert, J., Jacques-Coper, M., Van Daele, M., Urrutia, R., and Grosjean, M.: A 600 years warm-season temperature record from varved sediments of Lago Plomo, Northern Patagonia, Chile (47° S), Quaternary International, 377, 28–37, publisher: Elsevier, 2015.

Ericson, D. B., Ewing, M., Wollin, G., and Heezen, B. C.: Atlantic deep-sea sediment cores, Geological Society of America Bulletin, 72, 193–286, publisher: Geological Society of America, 1961.

Fischer, H. B., List, J. E., Koh, C. R., Imberger, J., and Brooks, N. H.: Mixing in inland and coastal waters, Academic press, 1979.

Garreaud, R., Lopez, P., Minvielle, M., and Rojas, M.: Large-Scale Control on the Patagonian Climate, Journal of Climate, 26, 215–230, https://doi.org/10.1175/JCLI-D-12-00001.1, 2012.

https://doi.org/10.5194/cp-2022-29
Preprint. Discussion started: 20 April 2022




Gornitz, V.: Paleoclimate Proxies, An Introduction, in: Encyclopedia of Paleoclimatology and Ancient Environments, edited by Gornitz, V., pp. 716–721, Springer Netherlands, Dordrecht, https://doi.org/10.1007/978-1-4020-4411-3_171, 2009.

Harris, I., Osborn, T. J., Jones, P., and Lister, D.: Version 4 of the CRU TS monthly high-resolution gridded multivariate climate dataset, Scientific Data, 7, 109, https://doi.org/10.1038/s41597-020-0453-3, bandiera_abtest: a Cc_license_type: cc_publicdomain Cg_type: Nature Research Journals Number: 1 Primary_atype: Research Publisher: Nature Publishing Group Subject_term: Atmospheric dynamics;Climate and Earth system modelling Subject_term_id: atmospheric-dynamics;climate-and-earth-system-modelling, 2020.

Helmke, J. P., Schulz, M., and Bauch, H. A.: Sediment-Color Record from the Northeast Atlantic Reveals Patterns of Millennial-Scale Climate Variability during the Past 500,000 Years, Quaternary Research, 57, 49–57, https://doi.org/10.1006/qres.2001.2289, publisher: Cambridge University Press, 2002.

Ibarzabal Y Donangelo, T., Hoffmann, J. A., and Naruse, R.: Recent climate changes in southern Patagonia, Bulletin of Glacier Research, pp. 29–36, 1996.

Imberger, J. and Patterson, J. C.: Physical Limnology, in: Advances in Applied Mechanics, edited by Hutchinson, J. W. and Wu, T. Y., vol. 27, pp. 303–475, Elsevier, https://doi.org/10.1016/S0065-2156(08)70199-6, 1989.

Ji, J., Shen, J., Balsam, W., Chen, J., Liu, L., and Liu, X.: Asian monsoon oscillations in the northeastern Qinghai–Tibet Plateau since the late glacial as interpreted from visible reflectance of Qinghai Lake sediments, Earth and Planetary Science Letters, 233, 61–70, https://doi.org/10.1016/j.epsl.2005.02.025, 2005.

Kristensen, P., Søndergaard, M., and Jeppesen, E.: Resuspension in a shallow eutrophic lake, Hydrobiologia, 228, 101–109, https://doi.org/10.1007/BF00006481, 1992.

Lenaerts, J. T. M., van den Broeke, M. R., van Wessem, J. M., van de Berg, W. J., van Meijgaard, E., van Ulft, L. H., and Schaefer, M.: Extreme Precipitation and Climate Gradients in Patagonia Revealed by High-Resolution Regional Atmospheric Climate Modeling, Journal of Climate, 27, 4607–4621, https://doi.org/10.1175/JCLI-D-13-00579.1, 2014.

Lewis, W. M.: Temperature, heat, and mixing in Lake Valencia, Venezuela, Limnology and Oceanography, 28, 273–286, https://doi.org/https://doi.org/10.4319/lo.1983.28.2.0273, _eprint: https://aslopubs.onlinelibrary.wiley.com/doi/pdf/10.4319/lo.1983.28.2.0273, 1983.

Lyell, S. C.: Principles of Geology: Being an Attempt to Explain the Former Changes of the Earth's Surface, by Reference to Causes Now in Operation, J. Murray, 1830.

Magnani, M. B., Fedotova, A., Peterson, D. E., and MacPhail, M. D.: Constraints on glacial isostatic adjustment in the Southern Patagonia Icefield from high-resolution seismic reflection imaging of glacial lacustrine deposits in the Lago Argentino, Argentina, AGU Fall Meeting Abstracts, 21, http://adsabs.harvard.edu/abs/2019AGUFM.C21F1516M, 2019.

Mann, M. E., Zhang, Z., Hughes, M. K., Bradley, R. S., Miller, S. K., Rutherford, S., and Ni, F.: Proxy-based reconstructions of hemispheric and global surface temperature variations over the past two millennia, Proceedings of the National Academy of Sciences, 105, 13 252–13 257, 2008.

McShane, B. B. and Wyner, A. J.: A statistical analysis of multiple temperature proxies: Are reconstructions of surface temperatures over the last 1000 years reliable?, The Annals of Applied Statistics, 5, 5–44, https://doi.org/10.1214/10-AOAS398, publisher: Institute of Mathematical Statistics, 2011.

Millan, R., Rignot, E., Rivera, A., Martineau, V., Mouginot, J., Zamora, R., Uribe, J., Lenzano, G., De Fleurian, B., Li, X., Gim, Y., and Kirchner, D.: Ice thickness and bed elevation of the Northern and Southern Patagonian Icefields, Geophysical Research Letters, p. 2019GL082485, https://doi.org/10.1029/2019GL082485, 2019.

https://doi.org/10.5194/cp-2022-29
Preprint. Discussion started: 20 April 2022




Minowa, M., Schaefer, M., Sugiyama, S., Sakakibara, D., and Skvarca, P.: Frontal ablation and mass loss of the Patagonian icefields, Earth and Planetary Science Letters, 561, 116 811, https://doi.org/10.1016/j.epsl.2021.116811, 2021.

Mouginot, J. and Rignot, E.: Ice motion of the Patagonian Icefields of South America: 1984–2014, Geophysical Research Letters, 42, 1441–1449, https://doi.org/10.1002/2014GL062661, 2015.

Nagao, S. and Nakashima, S.: The factors controlling vertical color variations of North Atlantic Madeira Abyssal Plain sediments, Marine Geology, 109, 83–94, https://doi.org/10.1016/0025-3227(92)90222-4, 1992.

National Research Council: Surface Temperature Reconstructions for the Last 2,000 Years, The National Academies Press, Washington, DC, https://doi.org/10.17226/11676, 2006.

Nederbragt, A. J., Dunbar, R. B., Osborn, A. T., Palmer, A., Thurow, J. W., and Wagner, T.: Sediment colour analysis from digital images and correlation with sediment composition, Geological Society, London, Special Publications, 267, 113–128, https://doi.org/10.1144/GSL.SP.2006.267.01.08, publisher: Geological Society of London, 2006.

Ortiz, J. D., Polyak, L., Grebmeier, J. M., Darby, D., Eberl, D. D., Naidu, S., and Nof, D.: Provenance of Holocene sediment on the Chukchi-Alaskan margin based on combined diffuse spectral reflectance and quantitative X-Ray Diffraction analysis, Global and Planetary Change, 68, 73–84, https://doi.org/10.1016/j.gloplacha.2009.03.020, 2009.

Reed, J. A.: The paleontological stratigraphic interval construction and analysis tool, publisher: Digital Repository@ Iowa State University, http://lib. dr. iastate. edu/, 2007.

Richter, A. J., Marderwald, E. R., Hormaechea, J. L., Mendoza, L. P. O., Perdomo, R. A., Connon, G. C., Scheinert, M., Horwath, M., and Dietrich, R.: Lake-level variations and tides in Lago Argentino, Patagonia: insights from pressure tide gauge records, publisher: Cnr Ist Italiano Idrobiologia, 2016.

Roth, S. and Reijmer, J. J. G.: Holocene millennial to centennial carbonate cyclicity recorded in slope sediments of the Great Bahama Bank and its climatic implications, Sedimentology, 52, 161–181, https://doi.org/10.1111/j.1365-3091.2004.00684.x, _eprint: https://onlinelibrary.wiley.com/doi/pdf/10.1111/j.1365-3091.2004.00684.x, 2005.

Schuttenhelm, R. T. E.: Geoscience investigations of two North Atlantic abyssal plains: the Esope International Expedition, Office for Official Publications of theEuropean Communities, 1989.

Spigel, R. and Imberger, J.: The classification of Mixed-Layer Dynamics of Lakes of Small to Medium Size, Journal of Physical Oceanography - J PHYS OCEANOGR, 10, 1104–1121, https://doi.org/10.1175/1520-0485(1980)010<1104:TCOMLD>2.0.CO;2, 1980.

Sprowl, D. R.: On the precision of the Elk Lake varve chronology, in: Elk Lake, Minnesota: Evidence for Rapid Climate Change in the North-Central United States, edited by Bradbury, J. P. and Dean, W. E., vol. 276, p. 0, Geological Society of America, https://doi.org/10.1130/SPE276-p69, 1993.

Sugiyama, S., Minowa, M., Sakakibara, D., Skvarca, P., Sawagaki, T., Ohashi, Y., Naito, N., and Chikita, K.: Thermal structure of proglacial lakes in Patagonia: Proglacial Lakes in Patagonia, Journal of Geophysical Research: Earth Surface, 121, 2270–2286, https://doi.org/10.1002/2016JF004084, 2016.

Sugiyama, S., Minowa, M., Fukamachi, Y., Hata, S., Yamamoto, Y., Sauter, T., Schneider, C., and Schaefer, M.: Subglacial discharge controls seasonal variations in the thermal structure of a glacial lake in Patagonia, Nature Communications, 12, 6301, https://doi.org/10.1038/s41467-021-26578-0, number: 1 Publisher: Nature Publishing Group, 2021.

Tian, J., Brown, T., and Hu, F.: Comparison of varve and 14C chronologies from Steel Lake, Minnesota, USA, Holocene, 15, 510–517, https://doi.org/10.1191/0959683605hl828rp, 2005.

https://doi.org/10.5194/cp-2022-29
Preprint. Discussion started: 20 April 2022




Tingley, M. P., Craigmile, P. F., Haran, M., Li, B., Mannshardt, E., and Rajaratnam, B.: Piecing together the past: statistical insights into paleoclimatic reconstructions, Quaternary Science Reviews, 35, 1–22, https://doi.org/10.1016/j.quascirev.2012.01.012, 2012.

Tylmann, W., Zolitschka, B., Enters, D., and Ohlendorf, C.: Laminated lake sediments in northeast Poland: distribution, preconditions for formation and potential for paleoenvironmental investigation, Journal of Paleolimnology, 50, 487–503, https://doi.org/10.1007/s10933-013-9741-7, 2013.

Van Wyk de Vries, M., Ito, E., Shapley, M., and Brignone, G.: Semi-automated counting of complex varves through image autocorrelation, Quaternary Research, 104, 89–100, https://doi.org/10.1017/qua.2021.10, publisher: Cambridge University Press, 2021.

Van Wyk de Vries, M., Ito, E., Shapley, M., Brignone, G., Romero, M., Wickert, A. D., Miller, L. H., and MacGregor, K. R.: Physical Limnology and Sediment Dynamics of Lago Argentino, the World's Largest Ice-Contact Lake, Journal of Geophysical Research: Earth Surface, 127, e2022JF006 598, https://doi.org/10.1029/2022JF006598, _eprint: https://onlinelibrary.wiley.com/doi/pdf/10.1029/2022JF006598, 2022.

von Gunten, L., Grosjean, M., Rein, B., Urrutia, R., and Appleby, P.: A quantitative high-resolution summer temperature reconstruction based on sedimentary pigments from Laguna Aculeo, central Chile, back to AD 850, The Holocene, 19, 873–881, https://doi.org/10.1177/0959683609336573, 2009.

Wei, J. H., Finkelstein, D. B., Brigham-Grette, J., Castañeda, I. S., and Nowaczyk, N.: Sediment colour reflectance spectroscopy as a proxy for wet/dry cycles at Lake El'gygytgyn, Far East Russia, during Marine Isotope Stages 8 to 12, Sedimentology, 61, 1793–1811, https://doi.org/10.1111/sed.12116, _eprint: https://onlinelibrary.wiley.com/doi/pdf/10.1111/sed.12116, 2014.

Wu, L., Wang, R., Krijgsman, W., Chen, Z., Xiao, W., Ge, S., and Wu, J.: Deciphering Color Reflectance Data of a 520-kyr Sediment Core From the Southern Ocean: Method Application and Paleoenvironmental Implications, Geochemistry, Geophysics, Geosystems, 20, 2808–2826, https://doi.org/10.1029/2019GC008212, _eprint: https://onlinelibrary.wiley.com/doi/pdf/10.1029/2019GC008212, 2019.

Zhang, Y. G., Ji, J., Balsam, W. L., Liu, L., and Chen, J.: High resolution hematite and goethite records from ODP 1143, South China Sea: Co-evolution of monsoonal precipitation and El Niño over the past 600,000 years, Earth and Planetary Science Letters, 264, 136–150, https://doi.org/10.1016/j.epsl.2007.09.022, 2007.